# Microring-resonator-based sensor measuring both the concentration and temperature of a solution

**Min-Suk Kwon,[1,*] and William H. Steier,[2]**

[1]*Department of Optical Engineering, Sejong University, 98 Gunja-dong, Gwangjin-gu, Seoul 143-747, Korea*
[2]*Department of Electrical Engineering, University of Southern California, 920 W. 37th PL, Los Angeles, CA 90089, USA*
[*]*Corresponding author: mskwon@sejong.ac.kr*

**Abstract:** We propose and investigate experimentally a micro-ring-resonator-based sensor with which we can measure both the concentration and temperature of glucose solution. It consists of two micro-ring resonators consecutively coupled to a bus waveguide by the overlap between them. The resonance wavelengths of the two resonators change similarly with the temperature but differently with the concentration. For that purpose, the core of just one micro-ring resonator is exposed directly to the solution. Using polymers, conventional processes, and a polymer lift-off process, we implement the sensor. Through the measurement of the fabricated sensor, we obtain its characteristics of measuring the temperature and concentration.



**OCIS codes:** (130.3120) Integrated optics devices; (130.5460) Polymer waveguides; (130.6010) Sensors; (230.5750) Resonators

## References and links

1. P. V. Lambeck, "Integrated optical sensors for the chemical domain," Meas. Sci. Technol. **17**, R93-R116, (2006).
2. X. D. Hoa, A. G. Kirk, and M. Tabrizian, "Towards integrated and sensitive surface plasmon resonance biosensors: A review of recent progress," Biosens. Bioelectron. **23**, 151-160 (2007).
3. M.-S. Kwon and S.-Y. Shin, "Refractive index sensitivity measurement of a long-period waveguide grating," IEEE Photon. Technol. Lett. **17**, 1923-1925 (2005).
4. P. Debackere, S. Scheerlinck, P. Bienstman, and R. Baets, "Surface plasmon interferometer in silicon-on-insulator: novel concept for an integrated biosensor," Opt. Express **14**, 7063-7071 (2006)
5. C.-Y. Chao, W. Fung, and L. J. Guo, "Polymer microring resonators for biochemical sensing applications," J. Sel. Top. Quantum Electron. **12**, 134-142 (2006).
6. A. Ksendzov and Y. Lin, "Integrated optics ring-resonator sensors for protein detection," Opt. Lett. **30**, 3344-3346 (2005).
7. W.-Y. Chen, V. Van, T. N. Ding, M. Du, W. N. Herman, and P.-T. Ho, "Benzocyclobutene negative-gap micro-ring notch filters," in *Frontiers in Optics*, OSA Technical Digest Series (Optical Society of America, 2005), paper SWA6.
8. BeamPROP™ is available from RSoft, Inc., http://www.rsoftinc.com.
9. B. Bhola and W. H. Steier, "A novel optical microring resonator accelerometer," IEEE Sens. J. **7**, 1759-1765 (2007).
10. P. Rabiei, W. H. Steier, C. Zhang, and L. R. Dalton, "Polymer microring filters and modulators," IEEE J. Lightwave Technol. **20**, 1968-1975 (2002).

## 1. Introduction

The bio-technology has been at the center of active research for recent years as problems related to health, safety, and the environment have become more and more important. For the development of the bio-technology, it is essential to make compact and sensitive sensors to detect a very small volume of a specific bio or chemical species. Integrated-optical sensors satisfy such a goal and have several other advantages such as immunity to electromagnetic interference and compatibility to microfluidic or electronic devices [1]. Based on surface plasmon polariton, long-period grating, interference, or resonance, they have been implemented [2-5]. Among them, microring-resonator (MRR) -based sensors have attracted

#93733 - $15.00 USD Received 12 Mar 2008; revised 3 Jun 2008; accepted 8 Jun 2008; published 11 Jun 2008

lots of attention since they are very small and sensitive as compared to others. MRR sensors detecting bulk refractive index change or a specific bio or chemical analyte after special surface treatment have been reported recently [5-6]. However, unfortunately, the high sensitivity of MRR sensors means that their characteristics also change sensitively with temperature. In order to remove the influence of a temperature change, in the previous works, MRR sensors were characterized with temperature held constant, which requires additional devices like a thermo-electric cooler. Therefore, it is necessary to develop MRR sensors which are not affected by a temperature change or which can separate its influence.

In this paper, we propose and investigate experimentally a MRR-based sensor measuring both the concentration and temperature of glucose solution. In the following sections, we describe its operation principle and fabrication. Then, we present experimental results and discussion. Finally, concluding remarks follow.

## 2. Description of the sensor

The proposed sensor consists of two MRRs with the same radius *R* coupled consecutively to a bus waveguide. Its schematic diagram is shown in Fig. 1(a). The cores of the MRRs and the bus waveguide are in the form of a square channel on a substrate as shown in Fig. 1(b). The two MRRs are sufficiently apart from each other such that there is no interaction between them. Obviously, they should be different for the measurement of two physical parameters. For that purpose, the core of MRR 1 is covered by a cladding, but the most part of the core of MRR 2 is uncovered. When the sensor is dipped into glucose solution, the uncovered core of MRR 2 contacts directly it.

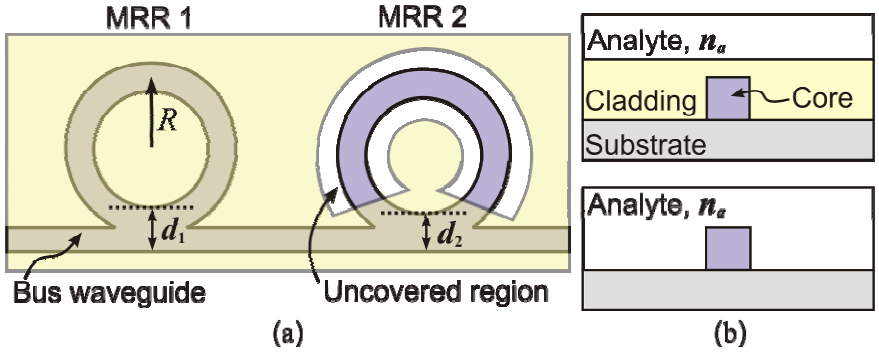


Fig. 1. (a). Schematic diagram of the proposed sensor, (b) waveguide structures of MRR 1 (top) and 2 (bottom).

As shown in Fig. 1(a), the coupling between the MRRs and the bus waveguide is achieved by overlapping them appropriately [7]. Usually, it has been obtained from the directional coupling mechanism. However, as well known, the gap between the MRR and the bus waveguide of a MRR device employing the latter becomes smaller as the index difference between the core and the cladding of the device increases. Consequently, it becomes harder to fabricate such a device using a conventional photolithography process. In contrast, the overlap-based coupling mechanism removes the difficulty in fabrication. This is because there is no need to pattern lines with sub-micrometer spacing for a MRR device based on it. The efficiency of the coupling between the MRR and the bus waveguide of such a device is easily controlled by adjusting the degree of overlapping. Using the finite-difference semi-vectorial beam propagation method [8], we simulated a structure comprised of straight and bent waveguides shown in Fig. 2(a). In the simulation, the refractive indexes of the core, the cladding, and the substrate were 1.567, 1.49, and 1.45, respectively. In addition, the width and height of the core were 2 and 2 μm, respectively, and the cladding was sufficiently thick. The radius of curvature of the bent waveguide was 1000 μm. Figure 2(b) shows the efficiency of coupling to the bent waveguide and that of transmission through the straight waveguide as functions of the gap defined in Fig. 2(a). The coupling efficiency takes almost all the values

#93733 - $15.00 USD Received 12 Mar 2008; revised 3 Jun 2008; accepted 8 Jun 2008; published 11 Jun 2008

between 0 and 1 as the gap decreases from 2 to 1 μm. The simulation results show that we can obtain a desired coupling efficiency using the overlap-based coupling mechanism although it changes sensitively depending on the degree of overlapping.

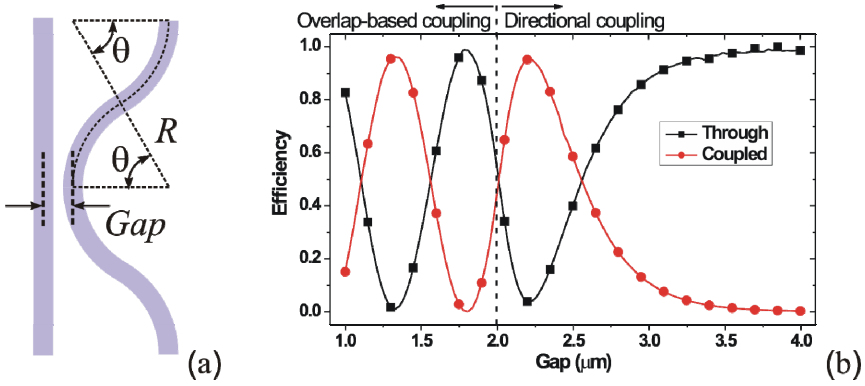


Fig. 2. (a). Simulated structure. In the simulation, θ = 11.5°. The gap between the straight and bent waveguides is defined as the distance between their centers. (b) Simulated efficiency of coupling to the bent waveguide and that of transmission through the straight waveguide.

The transmission spectrum through the bus waveguide of the proposed sensor has two distinct groups of resonance bands whose center wavelengths are given by $\lambda_{c,i} = 2\pi R N_{eff,i} / m_i$, where $i$ is 1 and 2 for MRR 1 and 2, respectively. In this equation, $N_{eff,i}$ is the effective index of a MRR mode, and $m_i$ is an integer. From this expression, a center wavelength change $\Delta\lambda_{c,i}$ is obtained as follows:

$$\Delta\lambda_{c,i} = \frac{2\pi R}{m_i}\left(\frac{\partial N_{eff,i}}{\partial n_a}\Delta n_a + \frac{\partial N_{eff,i}}{\partial T}\Delta T + \frac{\partial N_{eff,i}}{\partial \lambda}\Delta\lambda_{c,i}\right), \tag{1}$$

where $T$ and $n_a$ denote the temperature and refractive index of analyte, i.e. glucose solution, respectively. If we assume that $(2\pi R / m_i)\cdot(\partial N_{eff,i} / \partial\lambda) \ll 1$ and that $n_a$ is proportional to glucose concentration $C$, then Eq. (1) becomes

$$\begin{bmatrix}\Delta\lambda_{c,1}\\ \Delta\lambda_{c,2}\end{bmatrix} = \begin{bmatrix}S_{C,1} & S_{T,1}\\ S_{C,2} & S_{T,2}\end{bmatrix}\begin{bmatrix}\Delta C\\ \Delta T\end{bmatrix}, \tag{2}$$

where $S_{C,i}$ and $S_{T,i}$ are the change rates of a center wavelength related to MRR $i$ with respect to the concentration and the temperature, respectively. Through the characterization of the sensor, $S_{C,i}$ and $S_{T,i}$ are determined experimentally. Using them and Eq. (2), we can find out $\Delta C$ and $\Delta T$ after measuring $\Delta\lambda_{c,i}$.

### 3. Fabrication and measurement

To implement the proposed sensor, we used a $SiO_2$-deposited silicon wafer as a substrate. SU-8 (Microchem Corporation) was used as a core material. Using conventional processes, we made SU-8 patterns. First, we spin-coated SU-8 on the $SiO_2$ layer at 2100 rpm for 30 seconds. Then, it was pre-baked on a hot plate at 65 °C for 2 minutes, and soft-baked at 95 °C for 3 minutes. After the soft baking, we made the patterns of the MRRs and the bus waveguide with a mask aligner (MJB3, SUSS MicroTec Inc.). At this step, exposure energy measured at the wavelength of 405 nm was 70 mJ/cm$^2$. The exposed SU-8 layer was post-baked sequentially

#93733 - $15.00 USD Received 12 Mar 2008; revised 3 Jun 2008; accepted 8 Jun 2008; published 11 Jun 2008

at 65 °C for 2 minutes and at 95 °C for 3 minutes. Finally, it was developed in SU-8 developer, rinsed with isopropyl alcohol, and dried with nitrogen gas. The height and width of a formed SU-8 pattern were almost 2 and 2 μm, respectively. According to a simulation, the channel waveguide of this size supports two higher-order modes, which are near cut-off, as well as a fundamental mode.

For the most part of the SU-8 pattern for MRR 2 to be uncovered by a cladding, we used a polymer lift-off process. This process was done as follows. Over the core region of MRR 2 required to be uncovered, an 18-μm-thick ∩-shaped AZ P4620 (Clariant Co.) pattern was made. To make the pattern, we spin-coated AZ P4620 at 1000 rpm for 60 seconds, and baked on a hot plate at 110 °C for 1 minute. Then, the pattern was formed by a photolithography process, and developed in a mixture of 1 part AZ 400K (Clariant Co.) and 3 parts DI water (by volume). After making the AZ P4620 pattern, we spin-coated UFC170A (Uray Co.) used as a cladding and UV-cured it. Dipping the sample into AZ 400K, we removed the AZ P4620 pattern, and we baked the sample at 160 °C for 2 hours. Finally, using a dicing process, we prepared the input and output facets of the sensor. The size of the accomplished sensor chip was 8×8 $mm^2$.

A microscope image of the fabricated MRR 2 is shown in Fig. 3(a). In Fig. 3(a), thin lines correspond to the SU-8 patterns for the MRR and the bus waveguide. A Cross-section image of MRR 2 are shown in Fig. 3(b). As shown in Fig. 3(b), the cladding is thickest at the boundaries of the uncovered region of MRR 2, and it becomes gradually thinner as the distance from the region increases. The thickness of the cladding on the core of MRR 1 was 3 μm. In the fabricated sensor, both MRR 1 and 2 had a radius of 1000 μm. The gaps for MRR 1 and 2 were 1.4 and 1.5 μm, respectively, so $d_1$ and $d_2$ in Fig. 1(a) were 3.4 and 3.5 μm.

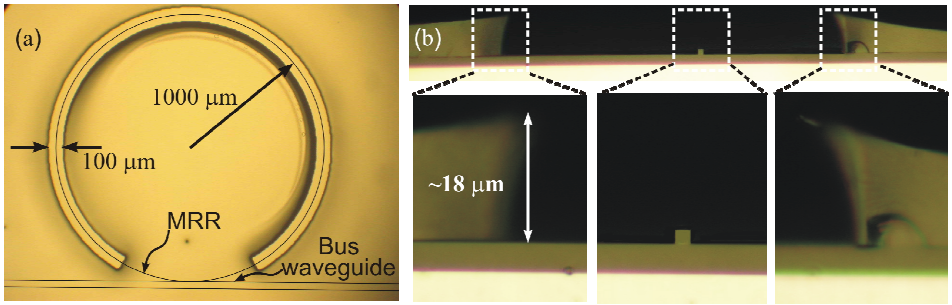


Fig. 3. Images of the fabricated sensor: (a) the top view of MRR 2, and (b) the cross-section of MRR 2.

For the characterization of the sensor, we pigtailed small-core fibers with a core diameter of 4 μm to the input and output facets, using glass ferrules and UV-curable epoxy [9]. As a light source, we used a tunable laser (Model 6200, New Focus Co.), and monitored the signal from the output fiber with a photo-detector. Dissolving $w_1$-gram glucose (G7528, Sigma Aldrich Co.) into $w_2$-gram DI water, we prepared glucose solution with the concentration $C = 100 \cdot w_1/(w_1+w_2)$ (%). Into the prepared glucose solution with a volume of about 1 litter, we dipped the pigtailed sensor, and measured its transmission spectrum while controlling the temperature of the solution.

## 4. Results and discussion

The measured transmission spectrum of the sensor dipped into pure DI water at 22 °C was shown in Fig. 4(a). As explained above, there are two groups of resonance bands corresponding to MRR 1 and 2. To check the resonance characteristics of a single MRR device based on the overlap-coupling mechanism, we made separately the same MRR device as MRR 1 and measured its transmission spectrum. A resonance band in the transmission spectrum was centered at 1310.987 nm, and its full width at half maximum (FWHM) was 40 pm. The free spectral range (FSR) measured around the resonance band was 166 pm, and the

#93733 - $15.00 USD Received 12 Mar 2008; revised 3 Jun 2008; accepted 8 Jun 2008; published 11 Jun 2008

calculated loaded Q of the MRR device was 33000. Among the resonance bands in Fig. 4(a), we tracked those centered at 1312.288 and 1312.249 nm related to MRR 1 and 2, respectively. Figure 4(b) shows changes in the spectrum which were observed as the concentration increased by 1.5 % or the temperature increased by 1 °C. Since SU-8 has a large thermo-optic coefficient and light is strongly confined to the SU-8 core, the effective indexes of the MRR modes decrease with the temperature, and so the resonance bands blue-shift. In contrast, the effective indexes increase with the concentration, and they red-shift. As shown below, MRR 1 and 2 have different temperature-dependent responses. Hence, the two resonance bands separate further with the increase of 1 °C.

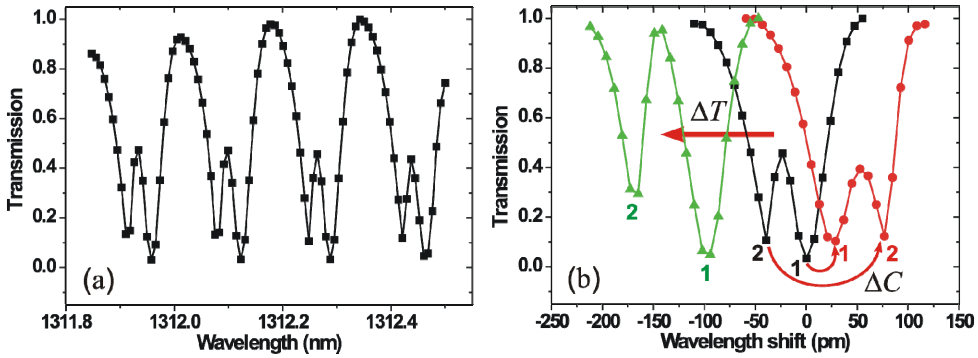


Fig. 4. (a). The measured transmission spectrum of the sensor dipped into pure DI water at 22 °C. (b) Changes of the transmission spectrum due to a temperature increase of 1 °C (the green line with triangles) and a concentration increase of 1.5 % (the red line with circles). Each number means that the resonance band corresponds to the MRR with the number.

Figures 5(a) and 5(b) show the center wavelength changes $\Delta\lambda_{c,1}$ and $\Delta\lambda_{c,2}$ related to MRR 1 and 2, respectively, as functions of the concentration for several temperatures. Data points in the graphs deviate somewhat from a linear relation since there was an inaccuracy of ± 0.5 °C in measuring temperature with a simple alcohol thermometer. The measured $S_{C,1}$ and $S_{C,2}$ were 35.2±7.11 and 98.3±8.19 pm/%, respectively. Using the ratio of the refractive index change of a glucose solution to its concentration change, which is ~$1.4\times10^{-3}$ RIU/%, we deduce that $S_{C,1}$ and $S_{C,2}$ can be converted to 25.1±5.08 and 70.2±5.85 nm/RIU, respectively. $S_{C,1}$ was larger than expected. This may be due to the diffusion or penetration of the glucose solution through the cladding. The value of $S_{C,2}$ is comparable to the previously reported value of about 105 pm/%, which was measured around the wavelength of 1550 nm [5].

The center wavelength changes $\Delta\lambda_{c,1}$ and $\Delta\lambda_{c,2}$ are shown as functions of the temperature for several concentrations in Figs. 6(a) and 6(b), respectively. The measured $S_{T,1}$ and $S_{T,2}$ were –81.0±7.26 and –92.5±6.02 pm/°C, respectively. Light is more strongly confined to the core of MRR 2 than that of MRR 1 since the cladding over that has a larger refractive index than glucose solution. Thus, $|S_{T,2}| > |S_{T,1}|$. The absolute values of $S_{T,1}$ and $S_{T,2}$ are a little smaller than the previously reported value of about 150 pm/°C, which was measured around the wavelength of 1550 nm [10].

As mentioned above, we can calculate and find $\Delta C$ and $\Delta T$ of unknown glucose solution, using Eq. (2) with the obtained values of $S_{C,1}$, $S_{T,1}$, $S_{C,2}$, and $S_{T,2}$ after measuring $\Delta\lambda_{c,1}$ and $\Delta\lambda_{c,2}$. The (1, 1), (1, 2), (2, 1), and (2, 2) elements of the inverse of the 2×2 matrix in Eq. (2) are –0.0197±0.0107 %/pm, 0.0172±0.0098 %/pm, –0.0209±0.0118 °C/pm, and 0.00749±0.0051 °C/pm, respectively. Because of the errors in these values, the calculated values of $\Delta C$ and $\Delta T$ may have quite large errors. Therefore, as a further work, it is required to measure carefully $S_{C,1}$, $S_{T,1}$, $S_{C,2}$, and $S_{T,2}$ with a more precise thermometer.

#93733 - $15.00 USD Received 12 Mar 2008; revised 3 Jun 2008; accepted 8 Jun 2008; published 11 Jun 2008

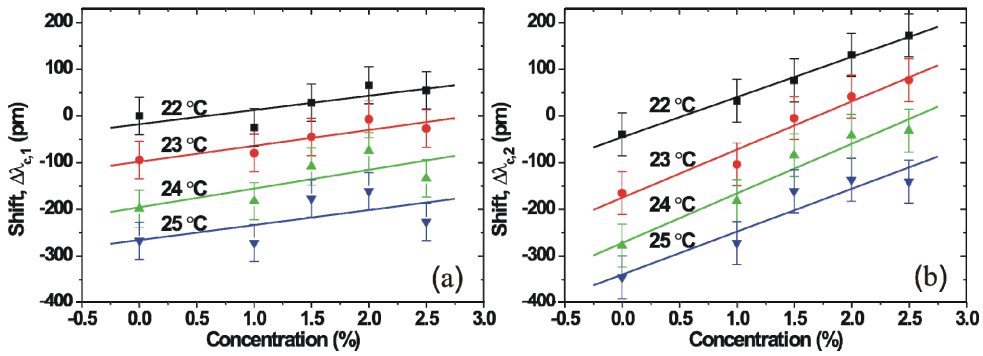


Fig. 5. Center wavelength changes (a) $\Delta\lambda_{c,1}$ and (b) $\Delta\lambda_{c,2}$ related to MRR 1 and 2, respectively, as functions of the concentration for several temperatures. The solid lines are obtained from linear fitting of the data. The error bars denote the inaccuracy of the wavelength shift inferred from that of measured temperature.

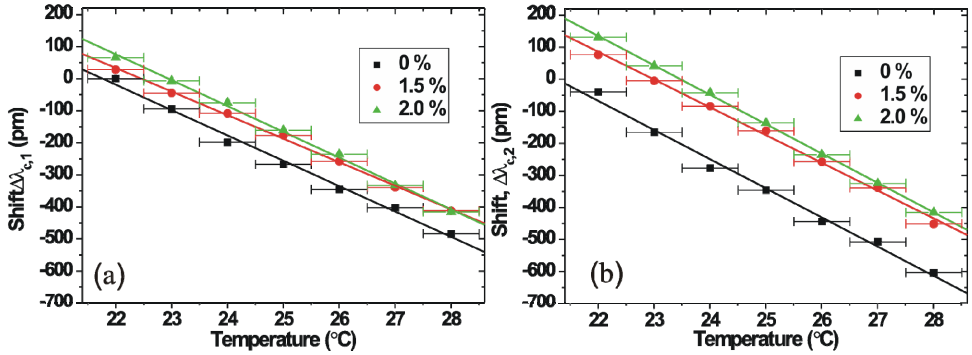


Fig. 6. Center wavelength changes (a) $\Delta\lambda_{c,1}$ and (b) $\Delta\lambda_{c,2}$ related to MRR 1 and 2, respectively, as functions of the temperature for several concentrations. The solid lines are obtained from linear fitting of the data. The error bars denote the inaccuracy in measuring temperature.

## 5. Conclusions

In summary, we proposed and implemented the sensor measuring both the concentration and temperature of glucose solution, which is based on the two MRRs consecutively coupled to the bus waveguide. It was made of polymer materials by using conventional processes and the lift-off process which is important in exposing selectively the core of one of the two MRRs. Through the measurement of the fabricated sensor, we determined the four change rates of center wavelengths related to the two MRRs with respect to the concentration and temperature of glucose solution. With these parameters, the sensor can be used to measure the concentration and temperature of given glucose solution. In this work, we had to immerse the sensor into glucose solution for measurement, which is slightly far from the concept of a compact and handy sensor. To solve this problem, a flow cell may be integrated onto the sensor. When such a flow-cell-integrated sensor is used, heat conduction from a solution through a silicon substrate may affect the temperature of the solution. To minimize the influence, a flow rate should be chosen carefully.

## Acknowledgment

The authors would like to thank Andrew Yick, Dr. Bipin Bhola, and Dr. Hidehisa Tazawa for helpful discussions about this work.

#93733 - $15.00 USD Received 12 Mar 2008; revised 3 Jun 2008; accepted 8 Jun 2008; published 11 Jun 2008